

Wind-driven circulation of Peninsular Malaysia's eastern continental shelf

ALEJANDRO CAMERLENGO and MONICA INES DEMMLER

Faculty of Applied Sciences and Technology, Universiti Putra Malaysia Terengganu,
Mengabang Telipot, 21030 Kuala Terengganu, Malaysia

ABSTRACT: In the course of this investigation, a nonlinear hydrodynamic, barotropic, numerical model for Peninsular Malaysia's eastern continental shelf has been developed. In the investigation, results of the wind driven ocean circulation are presented, with particular emphasis given to the ocean's response to the north-east (NE) and the south-west (SW) monsoon winds. Qualitatively, the results compare favorably with observations: the current flowing along the Vietnamese coast and along Peninsular Malaysia's east coast, during both monsoon seasons, is well resolved. The gyre on the South China Sea, is well resolved. It is shown that the existence of this gyre is only due to topographical effects. Quantitatively, our results, for the mass transports, along the Vietnamese coast and along Peninsular Malaysia's eastern continental shelf, are quite similar to the ones obtained in previous investigations.

Key words: Wind-driven marine circulation, Peninsula of Malaysia, Barotropic numerical model, Monsoon regime

RESUMEN: CIRCULACIÓN INDUCIDA POR EL VIENTO EN LA PLATAFORMA CONTINENTAL ORIENTAL DE LA PENÍNSULA DE MALASIA. – Se ha desarrollado un modelo numérico hidrodinámico, no lineal y barotrópico, para la plataforma continental oriental de la península de Malasia. Se presentan los resultados de la circulación inducida por el viento, con especial atención a la respuesta del océano a los monzones del noreste y suroeste. Cualitativamente los resultados coinciden bien con las observaciones: se resuelve bien la corriente que fluye a lo largo de la costa de Vietnam y a lo largo de la costa oriental de la península de Malasia durante ambos períodos monzónicos. También se resuelve bien el giro del Mar de la China del Sur. Se demuestra que la existencia de este giro debe únicamente a efectos topográficos. Cuantitativamente los resultados de transportes de masa a lo largo de la costa de Vietnam y de la plataforma oriental de la península de Malasia son muy similares a los obtenidos en estudios anteriores (Traducido por el Editor).

Palabras clave: Circulación marina inducida por el viento, Península de Malasia, Modelo numérico barotrópico, Régimen monzónico

INTRODUCTION

The aim of this investigation is to gain some understanding about the dynamics involved in the ocean circulation along Peninsular Malaysia's eastern continental shelf.

Over the past few years there has been an increased oil exploration activity in Peninsular Malaysia's eastern continental shelf. This activity is bound to grow even further in the next few years as new oil deposits had recently been discovered and with the consequent danger of a major oil spill catastrophe. Incidentally, oil spill accidents are frequent in the Malacca Straits. Malaysian research into different aspects of removal and containment of oil

*Received July 3, 1996. Accepted April 3, 1997.

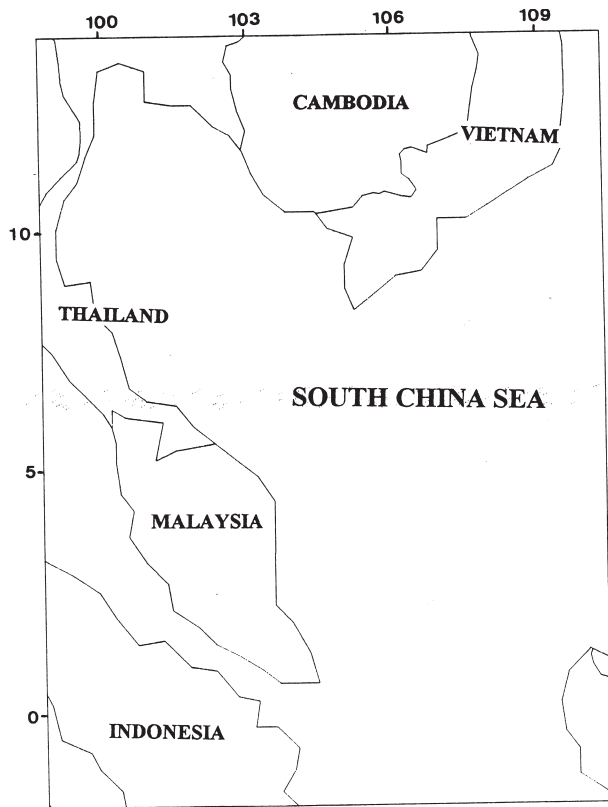


FIG. 1. Map showing the location of our region of concern in the South China Sea.

spill under adverse meteorological conditions, specially due to the NE monsoon, will necessarily have to undergo an accelerated expansion in the foreseeable future. And for this purpose an accurate knowledge of the ocean circulation will be crucial.

The origin of the expression monsoon is Arabic and means "season". This expression has been mainly used by the seamen, several centuries ago, to describe the semiannual reversal in the winds over the Arabian Sea (Das, 1992).

The climate of Peninsular Malaysia's east coast is affected by the monsoons. During the winter season, the air mass over Asia is cooler than in neighboring areas. Thus, a high pressure system is enhanced. On the other side, the air mass over Australia is warmer than in neighboring areas. A low pressure system over Australia is enhanced. The combined effect of these two pressure systems is a northeasterly wind over the South China Sea. This wind system is known as the Northeast monsoon wind.

On the other hand, during the northern summer, a high and a low pressure system over Australia and Asia; respectively, are enhanced. During the months

of May through September, these two pressure systems strengthen a southwesterly wind over the Southeast Asian region. This system is known as the southwest monsoon wind. Cloudless skies over the eastern coast of Peninsular Malaysia are observed during this period.

Two transitional periods (usually occurring during the months of April and October; respectively) are observed between these two monsoon seasons. These transitional periods, usually last for a period ranging from four to seven weeks.

Heavy rainfall in the east coast of the Peninsular Malaysia is usually associated with the northeast monsoon. The east coast is considered the wet belt of Peninsular Malaysia, with an annual rainfall of 2800 mm. Maximum precipitation usually occurs during the months of November and December (Chua, 1984).

The Somali Current has net mass transports and a current speed that exceed the Gulf Stream (Luther and Oí Brien, 1985). Because of the semiannual reversal in the wind system, there is also a reversal in the current flow in the upper layer of the ocean. The same process takes place in the South China Sea, particularly in our region of concern. However, the mass transport and the current speed along Peninsular Malaysia's east coast is somewhat less than the Somali Current.

Heavy precipitation and freshwater discharge from rivers, due to extreme rainfall, are one of the main characteristics of the NE monsoon season. The water mass, off the eastern coast of Peninsular Malaysia is characterized by its low salinity. Skies are overcast, thus preventing the warming of the sea surface by solar radiation. During this season a decrease in the sea surface temperature of approximately 1° C has been recorded. (Saadon and Camerlengo, 1995).

Due to the persistence of the NE winds the water mass tends to pile up against the western boundary causing an increase in the sea level. In fact, the sea level at the western boundary is higher than during any other time of the year (Saadon and Camerlengo, 1995).

The NE monsoon winds are much weaker than the SW monsoon winds in the Arabian Sea. The reverse is true in the South China Sea. Turbulence produced by strong winds mixes down the momentum input throughout the entire mixed layer (Niiler and Krauss, 1977). This is precisely what happens with the ocean mixed layer depth, at the western boundary during the NE monsoon season (Saadon and Camerlengo, 1995).

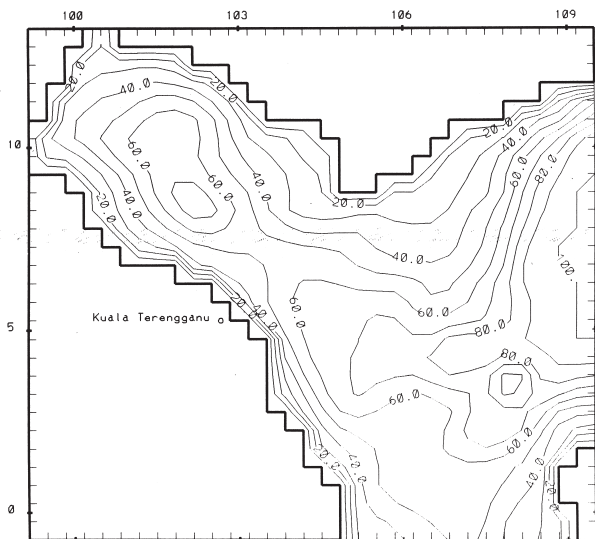


FIG. 2. Bathymetry (in meters) of the model region of the South China Sea.

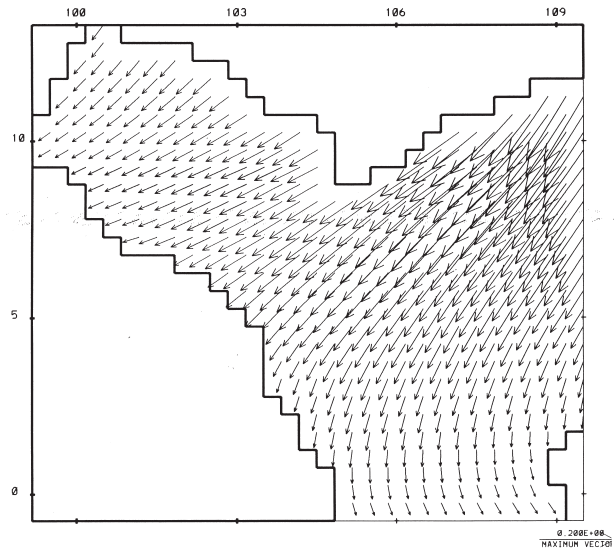


FIG. 3. Hellerman and Rosenstein's (1983) wind stress (in $N m^{-2}$) pattern for December.

During the SW monsoon season, cloudless skies cause an increase in both the salinity field and the temperature field patterns. A decrease of the mixed layer depth has also been recorded (Lokman *et al.*, 1986).

The region under consideration in this study is predominantly situated in the ASEAN region. Admittedly, the South China Sea has a very complex bottom bathymetry. However, the bottom topography of Peninsular Malaysia's eastern continental shelf has a moderate slope and progressively extends itself towards the South China Sea. The coastal areas are not profound.

Using mean summer (winter) monsoon winds, Pohlmann (1987) has simulated the circulation of the South China Sea and his numerical results compare reasonably well with Wyrtki's (1961) observations. Azmy *et al.* (1991) also has studied the numerical circulation, in our region of interest.

The aim of this study is to simulate the wind-driven circulation of Peninsular Malaysia's east coast. For this purpose, two typical months (of both the NE and the SW monsoon season; respectively) are chosen. Field observations in the South China Sea have been undertaken by Wyrtki (1961) and no significant improvement has been attained since then. Therefore, our model results are compared, both from a qualitative and a quantitative point of view, with Wyrtki's (1961) observations.

The model solves the barotropic, hydrodynamic, mode. Because of the fact that the wind-driven cir-

ulation is addressed, there is no need to implement a thermodynamic model. Therefore, the vertically integrated shallow water model is sufficient to accomplish this task.

No other undertaking has been made to simulate Peninsular Malaysia's eastern continental shelf. Hence, an increase in our knowledge of the dynamics involved in its circulation is very much needed.

THE MODEL

We have developed a wind-driven ocean numerical model to study the response of Peninsular Malaysia's eastern continental shelf ocean circulation to the NE and SW monsoon winds. The model solves the external, barotropic mode. The Boussinesq approximation and the hydrostatic pressure in the vertical is assumed.

The equations for the external mode are:

$$\frac{\partial u}{\partial t} + \frac{\partial(u^2/2)}{\partial x} + \frac{\partial(uv)}{\partial y} - fv = -g\partial\eta/\partial x + (T_x^w - T_x^b)/(\rho(D+\eta)) + K\Delta u$$

$$\frac{\partial u}{\partial t} + \frac{\partial(uv)}{\partial x} + \frac{\partial(v^2)}{\partial y} + fu = -g\partial\eta/\partial y + (T_y^w - T_y^b)/(\rho(D+\eta)) + K\Delta v$$

$$\frac{\partial\eta}{\partial t} + \frac{\partial(u(D+\eta))}{\partial x} + \frac{\partial(v(D+\eta))}{\partial y} = 0$$

where u and v are the vertically averaged velocity components in the x (east-west) and y (north-south)

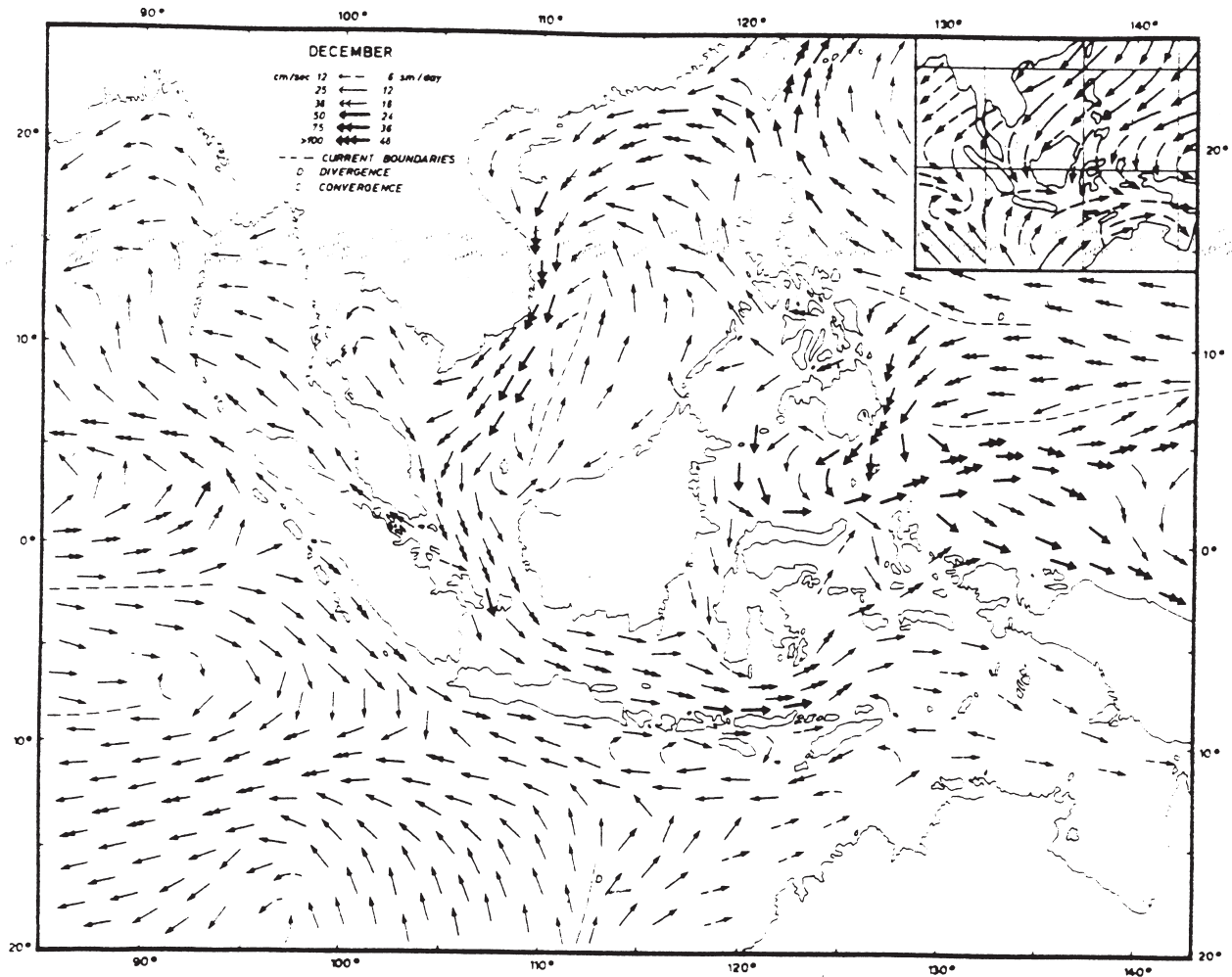


FIG. 4. Wyrтки's (1961) surface current chart and average wind pattern (upper right corner) for December.

directions, respectively; K ($= 100 \text{ m}^2 \text{ sec}^{-1}$, the horizontal kinematic eddy viscosity coefficient; g ($= 9.81 \text{ m}^2 \text{ sec}^{-1}$), the acceleration of the earth's gravity; D , the mean sea level; f , the Coriolis parameter; T , the external body force (where the superscript w (b) stands for the wind (bottom)); η , the free surface elevation; δ ($= 1020 \text{ kg} \cdot \text{m}^{-3}$, the sea water's density; and Δ , the horizontal Laplacian. The linear bottom friction is represented by:

$$(T_x^b, T_y^b) = r(u, v).$$

where r ($= 0.001$) represents the bottom friction coefficient.

The terms on the left hand side of the momentum equations represent the local time derivative, the nonlinear advective terms, and the Coriolis deflection term. The terms on the right hand side are, respectively, the pressure gradient due to the sloping

of the free surface, the tangential wind stress on the free sea surface, bottom friction and the horizontal momentum diffusion modeled empirically via an horizontal Laplacian operator.

The lattice where the model is being constructed is alternated in space: the C grid (Arakawa and Lamb, 1977). This particular grid has been used to avoid the noddling produced by the high wavenumbers.

The horizontal kinematic eddy viscosity coefficient is sometimes known as the sub-grid scale parameterization. We chose to keep it relatively small. The order of magnitude of the Laplacian (lateral viscous) terms are two or three orders of magnitude less than the leading terms of the momentum equation.

Hellerman and Rosenstein (1983) monthly wind stress forcing and a centered in space and time integration scheme are used. This particular scheme has the advantage of introducing no computational

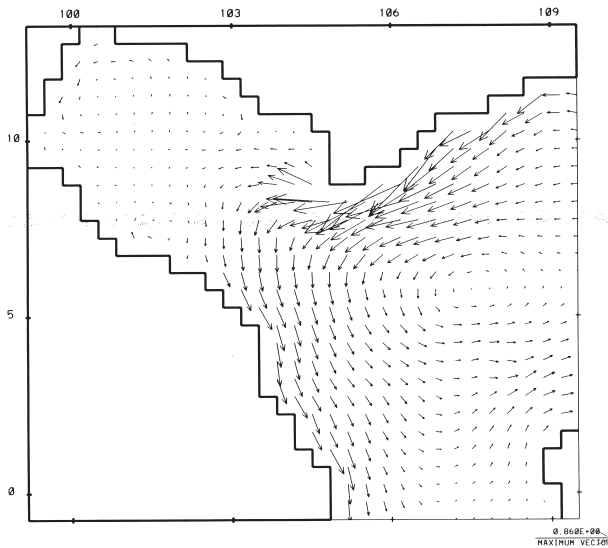


FIG. 5. – Model results for the South China Sea's December circulation (in m s^{-1}).

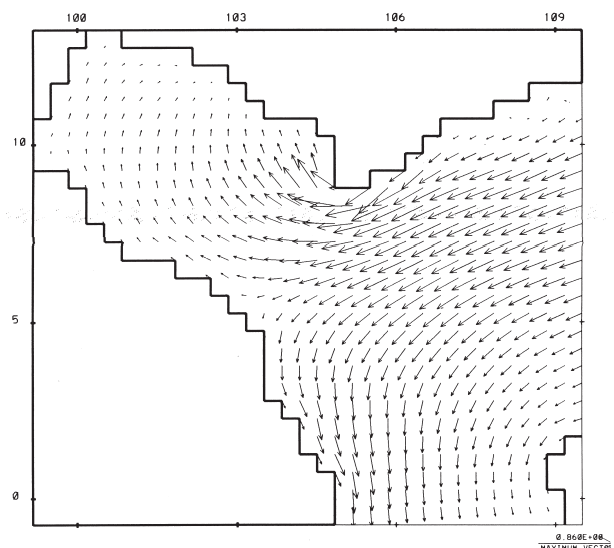


FIG. 6. – Idem as Fig. 5, but using an arbitrary flat bottom topography of 15 m.

damping to the physical solutions of the system (Camerlengo and O'Brien, 1980). It conserves mass and momentum to second order accuracy. A time step of 300 sec is used. The model starts from rest. Every $N (= 9)$ time level a Matsuno scheme is activated (Matsuno, 1966). Thus, the spurious computational mode is eliminated at every N time level.

The model extends from $99^{\circ} 10'$ E to $109^{\circ} 30'$ E in longitude and from $13^{\circ} 45'$ N to $0^{\circ} 30'$ S in latitude. The Cartesian grid spacing has $\Delta x = 37.5$ kms. and $\Delta y = 55.5$ kms. Therefore, 32 grid points are used in the east-west direction while 29 grid points are used in the north - south direction. This assumes to represent a distance of 1162.5 kilometers in the east-west direction and 1554 kilometers in the north - south direction (Fig. 2)

Solid walls are implemented at coastal boundaries where the normal velocity is set to be equal to zero. At the southern and eastern open boundaries, Camerlengo and O'Brien (1980) boundary conditions are implemented. The type of open boundary condition been implemented is a Sommerfield radiation equation, which was first implemented by Orlanski (1976). Different versions of this same type of OBC are currently being implemented (Guo and Zeng, 1995; Wheless and Klinck, 1995).

A stationary solution is reached within two days of integration. Because of the fact that no inflow of water is specified at the open boundaries, there is some loss of water mass. However, numerical verification of the total volume of water mass every time

step at all grid points, shows that the net water mass loss is negligible.

Bathymetric values are taken from the nautical chart of the British Admiralty numbers 2414 and 2660 A. The values taken from these charts represent an average depth for $\Delta x \Delta y$ square centered on the η grid point (Fig. 2) .

RESULTS AND DISCUSSION

No inflow of water mass is specified at the open boundaries. Therefore, the inflow of water mass, during the winter monsoon season, from the Pacific Ocean into the South China Sea through the Luzon Straits, is not specified at the eastern open boundary. Furthermore, the water mass entering the South China Sea through the Java Sea, at the southern boundary, during the summer monsoon, is not specified.

Roed and Cooper (1987) has shown that the interior solution may compare reasonable well with observations by tuning the bottom friction in the barotropic model. However, the numerical solution close to the open boundary may not be satisfactorily resolved as the numerical simulation of the interior domain. For this reason, the open boundary conditions has been placed further apart of our region of interest.

Typical values: $U = 0.1 \text{ m. s}^{-1}$; $L = 1000 \text{ km} = 10^6 \text{ m}$; (where U and L , represent the velocity and the

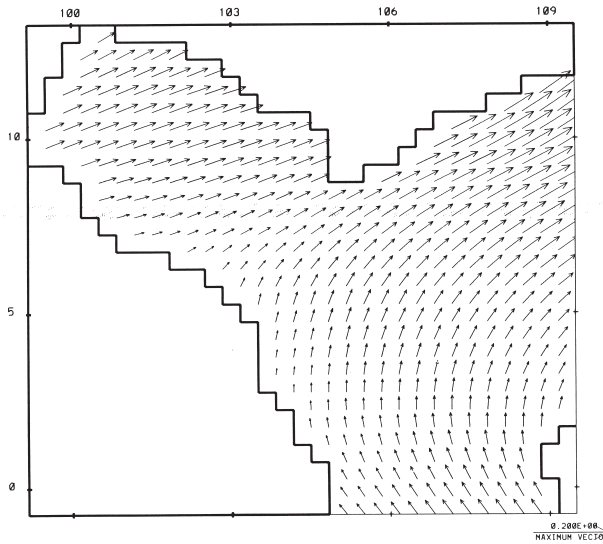


FIG. 7. – Idem as Fig. 3, but for August.

horizontal length scale; respectively) are taken. Upon considering an average latitude (of our area of concern) of 5° N, f is approximately 10^{-5} s^{-1} . Furthermore, the order of magnitude of η is roughly 0.1 m. In using these values, the scaling of the momentum equations shows that the three leading terms are the wind stress, the pressure gradient and the Coriolis terms. Therefore, the Coriolis deflection term, in our region of concern, still play an important role.

Following Wyrтки (1961), frictional terms will also be important in coastal areas, as well as the non-linear terms.

The oceans, in equatorial latitudes, adjust fast to changes in the wind pattern. The time it takes for a long Rossby wave, traveling at a speed C^* , to propagate a distance X^* , is known as the time of adjustment of the ocean (Philander, 1990). The time of adjustment, in equatorial latitudes, is roughly in the order of days.

The Indonesian Throughflow, via the Straits of Malacca, from the Pacific Ocean to the Indian Ocean is not significant (Wyrтки, 1961; Guoy, 1989). For this particular reason, a solid wall is placed all across the western boundary.

To better understand the dynamics of the circulation of the South China Sea, computer runs using a flat bottom topography have also been made.

NE Monsoon

Two periods are predominant: the winter monsoon and the summer monsoon. Strongest winds,

during the NE monsoon season, are recorded during December (Fig. 3). Surface currents, for December, are available (Fig. 4). Therefore, our study of the ocean's response to the NE monsoon winds will be related to this particular month (Fig. 5)

A maximum current flow is recorded along the Vietnamese coast during the NE monsoon season. An upslope of the free surface elevation towards the Vietnamese coast due to Ekman transport, is recorded. The current flow parallel to the Vietnamese coast, in the direction of the prevailing winds, is enhanced by geostrophy.

Due to Ekman transport, some of the water mass is deviated into the Gulf of Thailand. By continuity and due to coastal geometry, this water mass flows in a counter-clockwise rotation (Fig. 5). This type of motion has been confirmed by Wyrтки's (1961) observations (Fig. 4).

Whenever the NE monsoon blows towards the east coast of Peninsular Malaysia, an upsurge in the sea level is registered. This sea level rise has been simulated numerically by Azmy et. al. (1991). The authors attribute the discrepancy between their results with observed values, to the type of open boundary condition been implemented in their numerical model.

Therefore, during the winter monsoon, the water mass tends to pile up against Peninsular Malaysia's east coast. Due to the combined effects of coastal geometry, water mass flowing out of the Gulf of Thailand, and geostrophy, the water mass flows equatorwards, all along the western boundary.

In the northern hemisphere, the Ekman transport is at right angle of the prevailing winds. Therefore, upon arriving at Peninsular Malaysia's east coast, the water parcel is forced to move in a poleward direction, due to Ekman transport. This effect makes the current, flowing along our western boundary, to be somewhat of a smaller value than the current flowing along the Vietnamese coast. This feature has also been recorded by Wyrтки's (1961) observations (figs. 4 and 5).

It should be noted that our model is vertically integrated. The velocity field is representative of the whole water column. Therefore, given a similar wind stress all across the South China Sea, the shallower the water column (given a constant bottom friction coefficient), the greater the current flow representative of that particular vertical column. Thus, in our simulations, larger current flows are registered in coastal areas. Wyrтки's (1961) has studied in detail the surface current pattern. In spite of the dif-

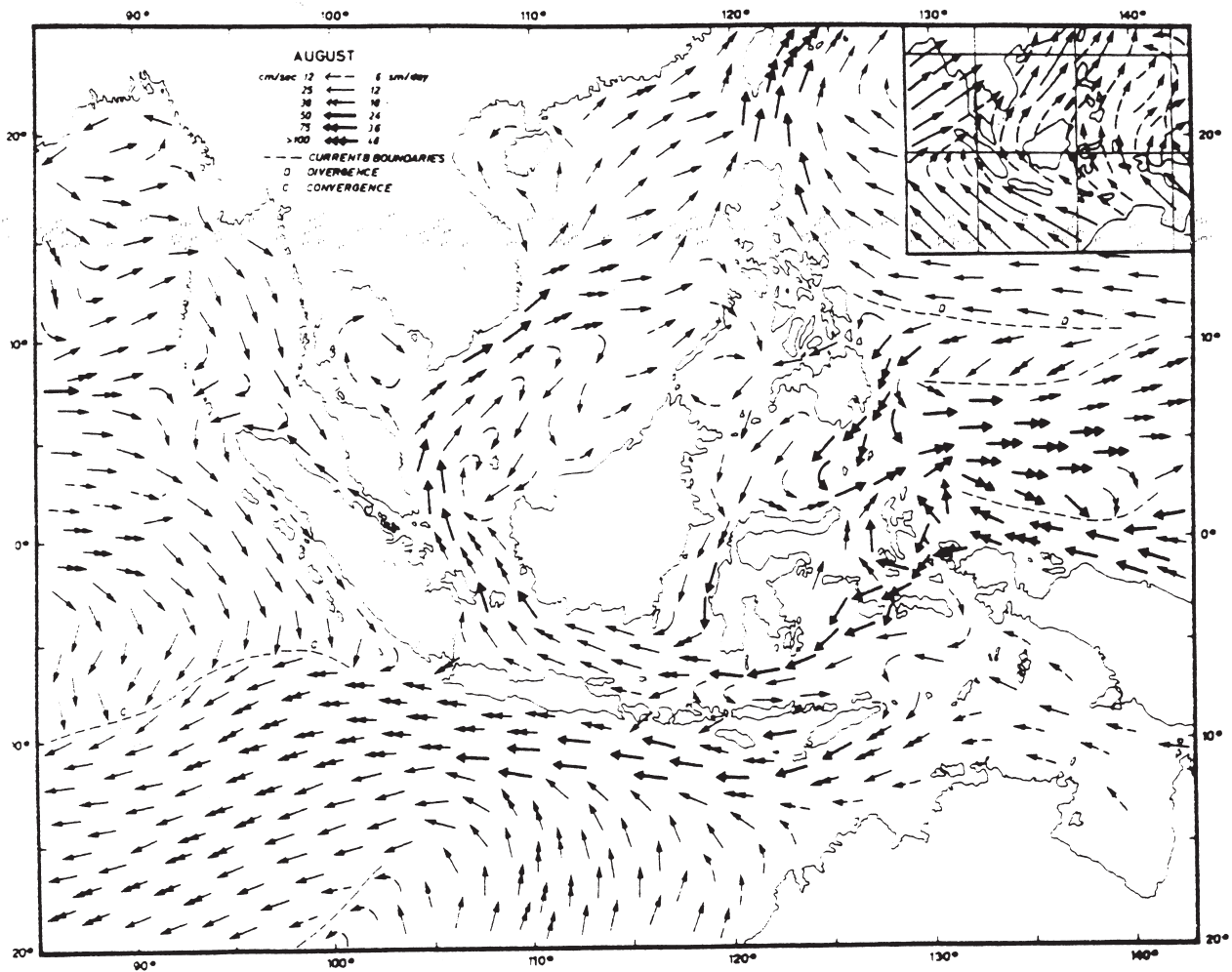


Fig. 8. Idem as Fig. 4, but for August.

ferent methodology being employed, our results are strikingly similar to Wyrki's in coastal areas. In coincidence with Wyrki's (1961) observations, a cyclonic gyre is well resolved in the South China Sea (Figs. 4 and 5). Our cyclonic gyre is embedded in a region where bottom topography is deep. Because of the nature of our vertically integrated model, our results of the current flow are of a somewhat less value than Wyrki's (1961).

Pohlmann's (1987) study only resolves this same eddy in the third layer (20 - 30 ms. deep) of his numerical simulation.

Computer runs made with a flat bottom do not resolve this cyclonic gyre. Therefore, the existence of this particular gyre is only due to topographical effects (Fig. 6).

To quantitatively compare our model results with Wyrki's (1961), the mass transport rates along the

Vietnamese coast and along Peninsular Malaysia's east coast, off Kuala Terengganu, are computed. Our results indicate that the mass transport for these two locations, for December, are 4.7 Sv. and 4.1 Sv., respectively. Wyrki's (1961, page 136) values, for this same month, are 5.0 Sv. and 4.0 Sv., respectively. In using a bottom friction coefficient, r , of 0.001 in our model simulation, our results compare favorable with Wyrki's.

The slight difference in the mass transport rates along the two coasts should be of no surprise since the current flow along the Vietnamese coast is greater than along Peninsular Malaysia's east coast.

SW Monsoon

Upon comparison of the mean wind stress of December and August, it can readily be inferred that

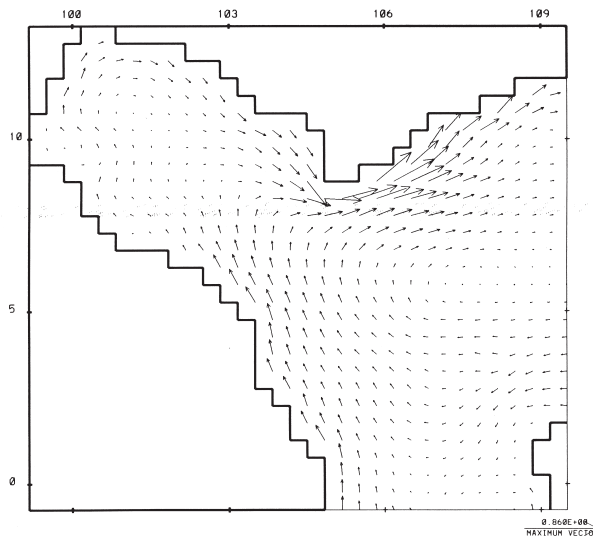


FIG. 9. – Idem as Fig. 5, but for August.

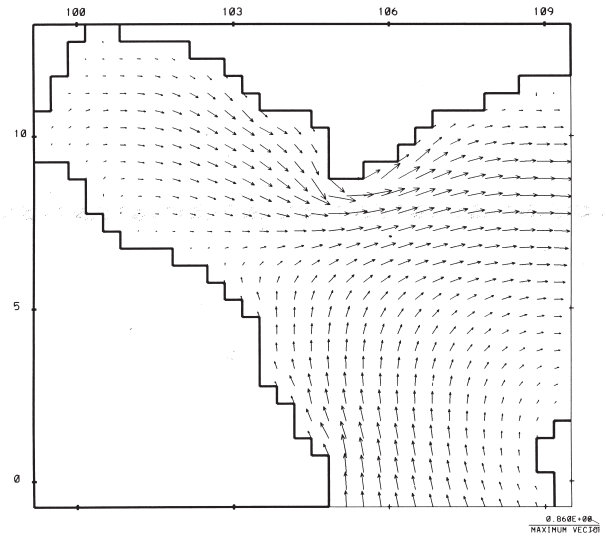


FIG. 10. – Idem as Fig. 6, but for August.

winds during the SW monsoon season are of a somewhat less value than its NE counterpart (Fig. 3 and 7). At the same time, the current flow is also inferior in August (Figs. 5 and 9).

The behavior of both the free surface elevation and the current flow for the months corresponding to the period of the SW monsoon season is quite similar. (Surface currents chart for August is available, Fig. 8). Thus, our study of the South China Sea's response to the summer monsoon winds is focused on this specific month.

Following Azmy *et al.* (1991), a depression of the free surface elevation at the western boundary is recorded. Concurrently, due to geostrophy a (secondary) maximum current flowing in a poleward direction along Peninsular Malaysia's east coast is also reported. Due to Ekman transport, this current flow is of a somewhat less value than the one that flows along the Vietnamese shores (Fig. 9).

Water mass, flowing northwards along Peninsular Malaysia's east coast, flows naturally into the Gulf of Thailand following a clockwise rotation. However, the bulk of the water mass, due to the combined effects of bottom topography and wind stress, will eventually flow towards the Vietnamese coast (Fig. 9).

A primary current flow along the Vietnamese coast is noticed (Fig. 9). Following Wyrтки (1961) and Pohlmann (1987), a decrease in the free surface elevation, in the order of ten centimeters, is also recorded. This decrease, is due to Ekman transport that drives water mass offshore the Vietnamese coast towards the South China Sea.

Water mass flowing out of the Gulf of Thailand (after completing its clockwise rotation) will eventually reinforce the current flow along the Vietnamese coast in the direction of the prevailing winds (Fig. 9).

In coincidence with observations, a gyre, located in the South China Sea, flowing in a clockwise rotation, is well resolved (Figs. 8 and 9). Due to the fact that the gyre is located over an area where bottom topography is relatively deep, our resolution of the current flow has a somewhat less value than Wyrтки's (1961). Pohlmann (1987) is able to resolve this same gyre in his numerical simulation of the South China Sea.

In the same fashion as for the NE monsoon case, a quantitative verification between our model results and Wyrтки's (1961) for August is done. Our results for the mass transport rates, along the Vietnamese coast and along our western boundary off Kuala Terengganu are 2.8 Sv. and 2.6 Sv., respectively. Wyrтки's (1961, page 136) values are 3.0 Sv for these two locations. Again, the coincidence between both set of results is auspicious.

The current flow along the Vietnamese coast is slightly greater than along Peninsular Malaysia's east coast (Fig. 9). However, the slope of the continental shelf off the Vietnamese coast has a somewhat lesser value than the slope of the continental shelf off the western boundary (Fig. 2). This explains the similar values for the mass transport rates for these two locations as reported by Wyrтки (1961).

In coincidence with our December results, computer runs been made using a flat bottom topography suggests that the existence of this gyre is only due to topographical effects (Fig. 10).

In general, a possible explanation for the discrepancies between observations and model results is that the model is forced using a monthly averaged wind stress. It is suspected that the interannual variability in the wind field may be important. Furthermore, fluctuations in the wind stress pattern on the time scale shorter than a month could have a significant effect in determining, e. g., the exact location of the gyre of the South China Sea.

SUMMARY AND CONCLUSIONS

NE winds are generally stronger than SW winds. Azmy et. al. (1991) show that the pile up of water during the winter monsoon along Peninsular Malaysia's east coast is greater than the lowering of the sea level during the summer monsoon. This effect is confirmed in our simulations.

It has been determined that the gyre located in the South China Sea, during both monsoon seasons is only due to topographical effects.

Qualitatively, we are able to simulate the NE and SW monsoons. The maximum currents the two flowing along the Vietnamese coast and along Peninsular Malaysia's east coast, respectively are well resolved.

Quantitatively, our model results show an auspicious agreement with observations. Our results for the mass transports rates off Vietnam and along Peninsular Malaysia's eastern continental shelf are quite similar to the ones of Wyrтки's (1961).

The model been used solves the barotropic mode. Thus, the current pattern represents the vertically averaged velocity. On the other hand, Wyrтки (1961) analyzes the surface current pattern. Therefore, there are bound to be differences. However, it should be stressed that both qualitatively and quantitatively the differences between our results and Wyrтки's are not significant.

ACKNOWLEDGMENTS

This investigation was financed by the Universiti Putra Malaysia. The authors gratefully acknowl-

edge this support. Assistance provided by Drs. T. Pohlmann and Nasir Saadon is fully appreciated.

REFERENCES

- Arakawa, A. and V. Lamb. – 1977. *Computational Design of the UCLA General Circulation Model. Methods of Computational Physics*, 17, Academic Press, New York.
- Azmy, A. R., Y. Isoda and T. Yanagi. – 1991. Sea Level Variations due to Wind around West Malaysia. *Memoirs of the Faculty of Engineering*, Ehime University, XII: 148-161.
- Camerlengo, A.L. and J.J. O'Brien. – 1980. Open Boundary Conditions in Rotating Fluids. *J. Comp. Physics*, 35: 12-35.
- Chapman, D. – 1985. Numerical Treatment of the Cross-Shelf Open Boundaries in a Barotropic Coastal Ocean Model. *J. Phys. Ocean.*, 15: 1050-1075.
- Chua, T.E. – 1984. Physical Environments of the East Coast of Peninsula Malaysia. In: Chua T.E. and J.K. Charles (eds.) Penerbit Univ. Sains Malaysia, Penang, pp. 1-10.
- Das, P.K. – 1992. *The Monsoons*. Third Edition. National Book Trust, India.
- Guo D.J and Q.C. Zeng. – 1995. Open Boundary Conditions for a Numerical Shelf Sea Model. *J. Comp. Phys.*, 116: 97-102.
- Gouy, T.K. – 1989. *Tides and Tidal phenomena of the ASEAN region*. M Sc. thesis. School of Earth Sciences, Flinders University of South Australia, Bedford Park, South Australia 5042.
- Hellerman, S. and M. Rosenstein. – 1983. Normal Monthly Wind-stress over the World Ocean with Error Estimates. *J. Phys. Ocean.*, 13: 1093-1104.
- Lokman, H., R. Yacoob and N.A.M. Shazili. – 1986. Some Measurements of Temperature and Salinity on a Portion of the South China Sea. In Ekspedisi Matahari 85. A Study of the Offshore Waters of the Malaysian EEZ. In: A.K. Mohsin, M.I. Mohamed and M.A. Ambak (eds.). Faculty of Fisheries and Marine Science, UPM. Occasional Publication No.3, pp. 49-79
- Luther, M.E. and J.J. O'Brien. – 1985. A Model of the Seasonal Circulation in the Arabian Sea Forced by Observed Winds. *Prog. Oceanog.*, 14: 353-385.
- Matsuno, T. – 1966. Numerical Integration of the Primitive Equations by a Simulated Backward Difference Method. *J. Meteor. Soc. Japan*, Ser. 2: 76-84.
- Niiler, P.P. and E.B. Kraus. – 1977. One Dimensional Models of the Upper Ocean. In: E.B. Kraus (ed.), *Modeling and Prediction of the Upper Layers of the Ocean*. Pergamon Press, pp. 143-172.
- Orlanski, I. – 1976. A Simple Boundary Condition for Unbounded Hyperbolic Flows. *J. Comp. Physics*, 21: 251-269.
- Philander, G. – 1990. *El Niño, La Niña, and the Southern Oscillation*. Academic Press.
- Pohlmann, T. – 1987. A Three Dimensional Circulation Model of the South China Sea. In: J. Nihouil and M. J. Jamart (eds.), *Three Dimensional Model of Marine and Estuarine Dynamics*, pp. 245-268. Elsevier Oceanographic Series. New York.
- Roed, L.P. and C.K. Cooper. – 1987. A Study of Various Open Boundary Conditions for Wind-forced Barotropic Numerical Ocean Models. In: J. Nihouil and M. J. Jamart (eds.), *Three Dimensional Model of Marine and Estuarine Dynamics*, pp. 305-336. Elsevier Oceanographic Series. New York.
- Saadon, M.N. and A. L. Camerlengo. – 1995. Response of the Ocean Mixed Layer, off the East Coast of Peninsula Malaysia during the Northeast and Southwest Monsoons. *Geoacta*, (Argentina) (in press).
- Wheless, G.H. and J.M. Klinck. – 1995. The Evolution of Density-Driven Circulation over Sloping Bottom Topography. *J. Phys. Ocean.*, 24: 888-901.
- Wyrтки, K.. – 1961. *Physical Oceanography of the Southeast Asian Waters*. NAGA Report vol. 2. University of California. La Jolla, USA.

Scient. ed.: J. Font